PART A2

PRODUCTION OF H,D(2s,2p) BY ELECTRON IMPACT (0 - 2000 eV) ON SIMPLE HYDROGEN CONTAINING MOLECULES

G.R. Möhlmann*, K.H. Shima+ and F.J. de Heer

FOM-Institute for Atomic and Molecular Physics, Kruislaan 407, Amsterdam/Wgm., The Netherlands

ABSTRACT

Absolute emission cross sections of Ly-α (H,D(2p → 1s)) radiation have been determined for 0 - 2000 eV electrons incident on H_2, HD, D_2, HCl, H_2O, NH_3 and CH_4. By mean of the application of electric quenching the excitation cross sections of H,D(2s) could be obtained from the increase of the resulting Ly-α radiation for these molecules. Only in the case of electrons on H_2, D_2 and HD excitation of H,D (2s) was found.

*Department of Theoretical Organic Chemistry, Leyden University, Leyden, The Netherlands.

+University of Hiroshima, Hiroshima, Japan.

TABLE 1

Summary of some previous investigations concerning Ly-α radiation produced by electrons on various molecules.

Group (ref.)	Compound	energy (eV)	abs σ_{em}	
			2s	2p
1	H, H_2	0 - 500		x
2	$CH_4, CD_4, C_2H_4, C_2H_6, C_6H_6$	50 - 6000	x	x
3	H_2, D_2	50 - 6000	x	x
4	H_2O	50 - 6000	x	x
5	CH_4	0 - 440		x
6	NH_3	0 - 480		x
7	H_2O	0 - 100		x
8	H_2	50 - 3000		x
9	H_2	50 - 6000		x
10	H_2O, NH_3, CH_4	0 - 300		x
11	$H_2, H_2O, D_2O, NH_3, CH_4, C_6H_6$	0 - 200		x
12	H_2	0 - 350		x
This work	$H_2, D_2, HD, HCl, H_2O, NH_3, CH_4$	0 - 2000	x	x

1. INTRODUCTION

Absolute emission cross sections (σ_{em}) of Ly-α radiation have been measured by several investigators [1 - 12] for electrons on various molecules such as H_2, D_2, H_2O, NH_3 and hydrocarbons. Their work has been summarized in table 1, with some details about the investigated parent molecules and the electron energies used.

The excitation cross sections (σ_{exc}) for H,D(2p) can be calculated from the σ_{em} (Ly-α)'s if a correction for cascade from higher lying H,D(ns,nd) levels is made. Vroom and de Heer [2 - 4] have reported σ_{exc}(H,D(2s)) values evaluated from the increase of the Ly-α radiation when an electric quenching field is applied. For the ratios of σ_{exc}(2s) and σ_{exc}(2p) they have found the values 0.5, 0.5, 0.1 and 0 respectively in the case of H_2, D_2, CH_4 and H_2O molecules, neglecting cascade effects. Cox and Smith [13] have measured σ_{exc} of D(2s) for electrons on D_2, using an rf field at the Lamb shift frequency. Misakian and Zorn [14] have investigated the angular distribution and the kinetic energies of H(2s) atoms produced by electron impact on H_2.

From the experimental results of Vroom and de Heer [2 - 4] and Cox and Smith [13] it appears that in the case of H_2 and D_2 a considerable fraction of the produced H,D(n = 2) atoms is in the 2s state. However, for other parent molecules refs. [2 - 4] contain 2s/2p cross section ratios which are small or even zero. Möhlmann et al. [15] have found that the H(3p) state is not produced by dissociative excitation of simple hydrogen containing molecules with electrons. Thus refs. [2 - 4,15] provide results which indicate that in many cases certain quantum states of H,D atoms are not formed in the electron impact dissociation process. To investigate this phenomenon in more detail for the H,D(n = 2) case, we have determined the 2s/2p cross section ratios for the target gases H_2, HD, D_2, HCl, H_2O, NH_3 and CH_4. This has been done by measuring the intensity of the Ly-α radiation with and without an electric quenching field for 100 - 2000 eV electrons incident on these gases.

2. EXPERIMENTAL

2.1. Apparatus

The experimental set up used in this experiment is basically the same as that described in ref. [15], however, with a different photon detection system.

The Ly-α photons are detected by a channeltron ultraviolet photon counter tube (Bendix, model no. BX 7600 - 4413) in combination with an oxygen filter, at an angle of 90^{o} to the electron beam. The filter is a gas cell with two lithium fluoride (LiF) windows, each 1.6 mm thick and at a mutual distance of 16.5 mm. It can be filled with oxygen gas reaching pressures between 0 and 500 Torr. The transmission properties of this optical detection system is discussed in section 2.2.

The detector was provided with a collimating system of two square slits so that it could "see" the radiation from an effective length of about 3.6 mm along the electron beam and about 8 mm on each side in a direction perpendicular to the electron beam and the beam-detector axis.

The electric field, used for the quenching of the H,D(2s) atoms, is applied parallel with the electron beam, as discussed in section 3 of ref. [15]. As shown there, the applied fields have no influence on the energy definition of the incident electrons at the observation region. Below 100 eV it is expected that the application of the electric field will influence the electron energy in the observation region considerably. Therefore no experiments have been performed with the field on for $E_{el} < 100$ eV.

The Ly-α emission intensities have been measured both as a function of the target gas pressure and the electron beam current. In the cases where a non-linearity was found an extrapolation towards zero pressure and/or beam current has been made.

For electron energies in the range 100 - 2000 eV no coaxial magnetic field has been used for the confinement of the electron beam. In the energy region 0 - 100 eV the magnetic field strength was 30 Gauss.

The target pressures have been measured with a capacitance manometer (MKS-Baratron, pressure head 77 H-1).

2.2. Properties of the photon detection system

According to the specifications of the manufacturer the Bendix photon tube used in this experiment has a maximum quantum yield of 9% around the Ly-α wavelength. Towards shorter wavelengths the transmission is cut-off at 1140 Å by the magnesium fluoride (MgF_2) multiplier window, whereas at longer wavelengths the yield decreases to 0.9% at 1800 Å and to 0.15% at 1900 Å. The transmission properties of oxygen have been given by Watanabe [16] and Friedmann [17]. At the Ly-α wavelength there is a window in the oxygen absorption spectrum, together with some windows around this wavelength and above 1795 Å.

As a consequence of the properties described above, our photon detection system will almost only detect Ly-α radiation from the emission spectra produced by electron impact on the molecules used in our experimental study.

From the emission spectra (1000 - 2000 Å) of Morgan and Mentall [10] produced by 100 eV electrons on H_2O, NH_3 and CH_4, we could determine that, for an oxygen pressure of 500 Torr in the filter, more than 99% of the transmitted radiation is Ly-α radiation.

In the case of H_2, Carriere and de Heer [18] showed that besides Ly-α a considerable amount of molecular H_2 radiation is transmitted through the LiF - O_2 filter. Using their experimental results, we have calculated that, in our set up and for an O_2 pressure of 500 Torr, 80% of the transmitted intensity is due to Ly-α radiation. No experimental data are available about the transmission of molecular HD and D_2 emissions through an LiF-O_2 combination. However for D_2 we can derive the transmission properties of our detector in the following way: Vroom and de Heer [3], using a vacuum monochromator, reported an isotope effect of about 20% for σ_{em}(Ly-α) in the case of 100 eV electrons incident on H_2 and D_2.

Experimentally, we have found that the signal from our LiF-O_2 multiplier combination for 100 eV electrons on D_2 was about 20% lower than the corresponding signal in the case of H_2; this latter H_2 signal had already been corrected for the 20% molecular H_2 contribution. So the above mentioned facts indicate that in the case of 100 eV electron impact on D_2 (almost) all molecular radiation is absorbed by the LiF-O_2 filter system. For HD we have assumed that about 10% of the transmitted radiation (500

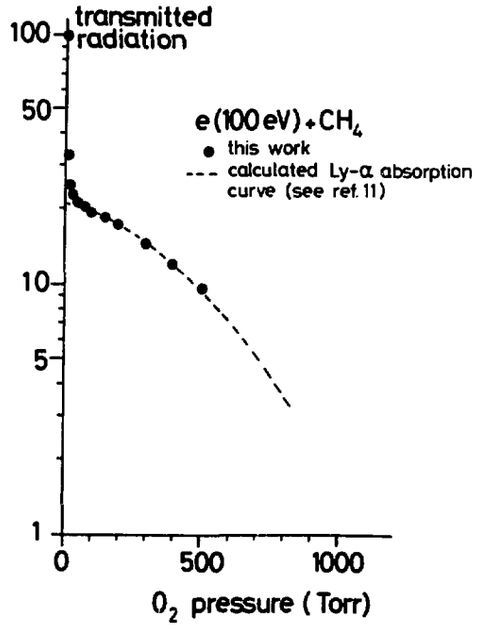

Fig. 1 - Transmitted vacuum ultra violet radiation versus the O_2 pressure in the LiF-O_2 filter for 100 eV electrons on CH_4.

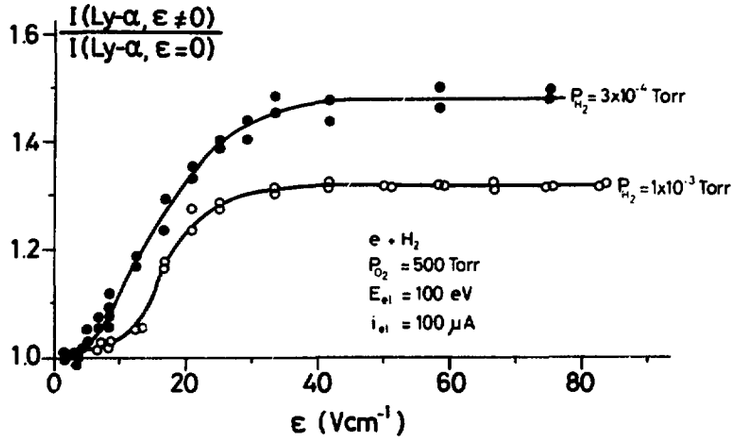

Fig. 2 - Quenching of the H(2s) state as a function of the electric field strength ε for two different H_2 pressures.

Torr O_2) is due to molecular emissions.

The O_2 filter has a window at the position of the ClI emission line at 1188.77 Å [16,17,19]. Therefore in the case of HCl the transmitted emission may contain some of this ClI radiation.

We have normalized our σ_{em} (Ly-α, $2p \rightarrow 1s$, H_2) at 100 eV impact energy to the value 12×10^{-18} cm^2 according to the discussion presented by Mumma and Zipf in section III.1 of their publication [12]. This σ_{em} value is close to that (11×10^{-18} cm^2) given by de Heer and Carriere [9].

3. EXPERIMENTAL PROCEDURE

3.1. Intensity of transmitted radiation versus the O_2 pressure in the filter

Fig. 1 shows the emission intensity of the total transmitted vacuum ultraviolet radiation (v.u.r.) between 1140 Å and about 1900 Å as a function of the O_2 pressure in the LiF-O_2 filter for 100 eV electrons on CH_4. For O_2 pressures in the range 0 - 100 Torr the transmitted intensity decreases drastically, whereas for pressures larger than 100 Torr the slope of the intensity curve becomes less steep. The intensity curve then coincides with a calculated transmission curve for Ly-α radiation by O_2 (and O_4) as derived using the results of Watanabe [16]. The measurement of the transmitted v.u.r. as a function of the O_2 pressure enables us to select a proper O_2 pressure to separate the Ly-α radiation from the remaining v.u.r. Only if some radiation other than Ly-α falls into an oxygen transmission window, the separation of the Ly-α radiation is not complete as is the case for H_2 and possibly for HCl.

For the other parent molecules used in this experiment similar O_2 pressure dependent intensity curves have been obtained.

The sensitivity of the detection system for Ly-α radiation is evaluated from the intensity measurement in the case of electrons on H_2 at 100 eV, for which the cross section for Ly-α emission is known (taking into account the correction for the contribution of the molecular H_2 radiation, see section 2.2).

TABLE 2

Emission cross sections ($10^{-18}cm^2$) for Ly-α radiation and 2s/2p cross section ratios at 100 eV electron impact energy.

com-pound	2p → 1s						2s → 1s			2s/2p	
	this work	refs. [2-4]	ref. [11]	ref. [10]	refs. [5-7]	ref. [9]	this work	refs. [2-4]	ref. [13]	this work	refs. [2-4]
H_2	12.0	13.1	11	-	-	11	7.26	6.35	-	0.605	0.485
HD	10.8	-	-	-	-	-	4.84	-	-	0.448	-
D_2	9.64	10.7	-	-	-	-	4.63	5.25	3.27	0.480	0.491
HCl	38.2	-	-	-	-	-	0	-	-	0	-
H_2O	19.3	32.3	9	8.8	7.5	-	0	0	-	0	0
NH_3	19.2	-	7	10.9	7.0	-	0	-	-	0	-
CH_4	12.1	12.4	14	1.2	2.45	-	0	1.3	-	0	0.105
CD_4	-	10.0	-	-	-	-	-	1.02	-	-	0.102

3.2. Application of the electric quenching field

If the Ly-α radiation intensity is measured when there are no external electric and/or magnetic fields, σ_{em} refers to that of the transition $2p \rightarrow 1s$ and we can write (neglecting the cascade):

$$\sigma_{em}(\text{Ly-}\alpha) = \sigma_{exc}(2p) \qquad (1)$$

By application of a (homogeneous) electric field the atomic H,D sublevels $^2S_{\frac{1}{2}}$ and $^2P_{\frac{1}{2}}$ are mixed [20]. The radiative transition probability for decay to the ground state of the former metastable $^2S_{\frac{1}{2}}$ state is a function of the applied electric field strength (ε) and has been calculated by Lüders [21]. This transition probability increases with increasing ε. For $\varepsilon = 80$ V cm^{-1} the radiative lifetime τ_{rad} has decreased to about 50 ns. Taking into account the high velocity (up to 40 km s^{-1} [14]) that the H atoms can have after the dissociative excitation process, τ_{rad} and the dimensions of the observation region, at least 99% of the former H,D (2s) atoms will decay by radiation within the observation region. When this is the case we can write (neglecting cascade):

$$\sigma_{em}(\text{Ly-}\alpha) = \sigma_{exc}(2s) + \sigma_{exc}(2p) \qquad (2)$$

So the difference in σ_{em}(Ly-α), in the case with and without the electric field, is due to the contribution of H,D (2s).

We have measured the Ly-α emission intensity I as a function of ε for 100 eV electrons on H_2. The result is shown in fig. 2 for two different H_2 pressures. For $\varepsilon \approx 3$ V cm^{-1} the Ly-α signal starts to increase and becomes saturated at about 40 V cm^{-1}. When the electric field was applied in the opposite direction the same result was obtained. It is seen in fig. 2 that the ratios $I(\text{Ly-}\alpha, \varepsilon \neq 0)/(\text{Ly-}\alpha, \varepsilon = 0)$ do not reach the same saturation value in the range $\varepsilon > 40$ V cm^{-1} for different H_2 target gas pressures. This pressure effect will be discussed in the next section.

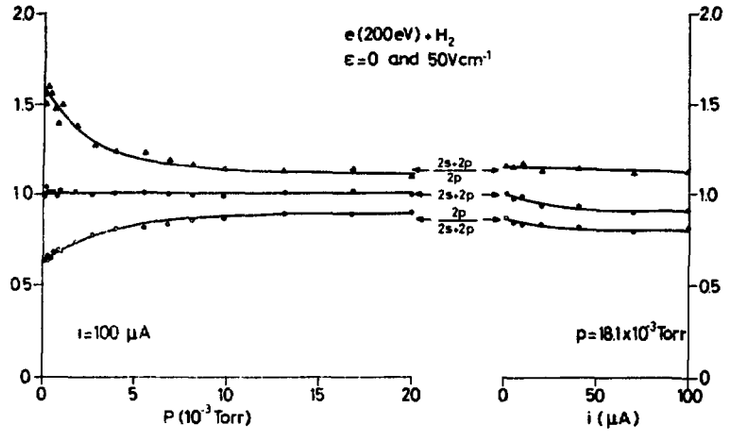

Fig. 3 - Influence of the H_2 target pressure and the electron beam current on the 2s/2p cross section ratio for 200 eV electrons on H_2 with electric field strength ε equal to zero and 50 V cm^{-1}.

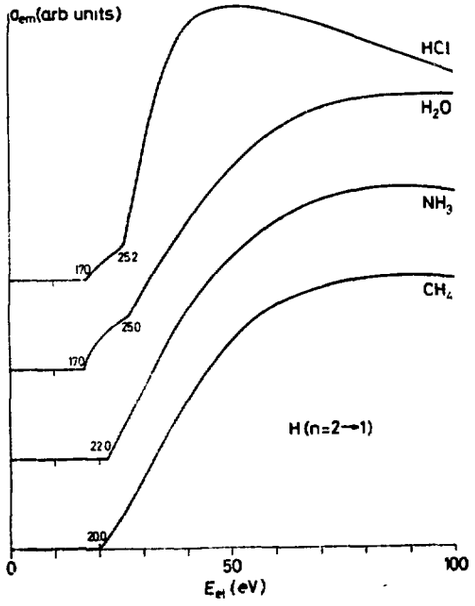

Fig. 4 - Ly-α excitation curves for 0 - 100 eV electrons incident on various molecules.

3.3. Influence of the H_2 target gas pressure and the electron beam current on the $I(Ly\text{-}\alpha, \varepsilon \neq 0)/I(Ly\text{-}\alpha, \varepsilon = 0)$ ratio

We have measured the Ly-α intensities (I(Ly-α)) as a function of the target gas pressure in the case with ($\varepsilon = 50$ V cm^{-1}) and without ($\varepsilon = 0$ V cm^{-1}) an electric field. In fig. 3 we have plotted the cross section ratios $(2s + 2p)/2p$ ($=I(Ly\text{-}\alpha, \varepsilon \neq 0)/I(Ly\text{-}\alpha, \varepsilon = 0)$) and $2p/(2s + 2p)$, together with the relative cross section sums $2s + 2p$, for electrons on H_2 in the pressure range $0 - 20 \times 10^{-3}$ Torr. As is seen in fig. 3 the cross section sum ($=I(Ly\text{-}\alpha, \varepsilon \neq 0)$) is independent of the H_2 target pressure. However the ratio $(2s + 2p)/2p$, which equals $2s/2p + 1$, is not constant but decreases for increasing H_2 pressure. This means that, due to the surrounding target gas molecules, the H(2s) atoms have already become less metastable.

The target gas pressure effect can be caused by collision ($H(2s) + H_2$) induced Ly-α radiation, or by the creation of an electric field due to the produced positive ions in the target gas (space charge effect). This latter effect should also be a function of the electron beam current. Therefore we have performed a beam current dependent measurement at a fixed H_2 pressure. At the right hand side of fig. 3 is seen that a variation of the beam current in the range 0 - 100 μA changes the $(2s + 2p)/2p$ ratio with a few percent only. Therefore the pressure effect is not due to the produced positive ions but to collisions between H(2s) and H_2. From our pressure dependent 2s/2p measurements we could estimate the cross section for the process:

$$H(2s) + H_2 \rightarrow H(1s) + H_2 + Ly\text{-}\alpha \qquad (3)$$

to be of the order of 1.5×10^{-15} cm^2.

The conclusion from the pressure dependence of $(2s + 2p)/2p$ is that the measurements must be carried out at low pressures to obtain reliable results for the 2s/2p ratio. In fig. 3 can be seen that in the case of H_2 for $p < 3 \times 10^{-4}$ Torr the error is less than 5%.

TABLE 3

Emission cross section of Ly-α radiation ($10^{-18}cm^2$ for electrons (0 - 2000 eV) incident on various molecules

eV	σ_{em} (2p → 1s)							σ_{em}(2s → 1s)		
	CH_4	NH_3	H_2O	HCl	H_2	HD	D_2	H_2	HD	D_2
20	0	0	2.05	3.07	-	-	-	-	-	-
30	3.09	5.02	5.50	25.6	-	-	-	-	-	-
40	6.66	10.7	10.2	47.8	-	-	-	-	-	-
50	9.34	14.8	14.1	51.2	-	-	-	-	-	-
60	11.0	17.3	16.8	49.1	-	-	-	-	-	-
70	11.7	18.8	18.3	46.7	-	-	-	-	-	-
80	12.1	19.4	18.8	44.7	-	-	-	-	-	-
90	12.2	19.8	19.2	42.0	-	-	-	-	-	-
100	12.1	19.3	19.2	38.2	12.0	10.8	9.64	7.26	4.84	4.63
150	10.1	16.7	18.1	30.6	9.71	9.22	7.90	5.73	4.00	3.79
200	8.21	13.9	15.6	26.1	8.19	7.70	6.46	4.75	3.34	3.03
300	5.62	10.2	12.0	18.3	6.51	6.05	4.53	3.97	2.60	2.21
400	4.11	7.50	10.1	14.6	5.29	4.80	3.64	3.12	2.09	1.80
500	3.11	5.93	8.02	12.0	4.40	3.98	3.01	2.55	1.79	1.42
600	2.59	4.77	7.14	10.0	3.75	3.44	2.54	2.25	1.56	1.22
700	2.16	4.08	6.17	8.86	3.22	3.02	2.27	1.93	1.36	1.07
800	1.84	3.75	5.49	7.86	3.00	2.73	2.04	1.74	1.25	1.00
900	1.58	3.26	4.95	6.79	2.76	2.48	1.89	1.63	1.14	0.906
1000	1.43	3.07	4.53	6.29	2.48	2.33	1.71	1.51	1.03	0.855
1200	1.19	2.44	3.85	5.16	2.10	1.96	1.45	1.28	0.871	0.711
1500	0.89	1.95	3.15	4.16	1.80	1.62	1.19	1.06	0.761	0.607
1700	0.84	1.77	2.82	3.59	1.56	1.47	1.08	0.920	0.683	0.529
2000	0.69	1.42	2.47	3.10	1.41	1.26	0.916	0.874	0.612	0.477

4. RESULTS

First we consider our data in the energy range 0 - 100 eV. The σ_{em}(Ly-α)'s, measured in the field-free case ($\varepsilon = 0$) and thus referring to $\sigma_{exc}(2p)$, are presented in table 2 for 100 eV electrons incident on various molecules.

By application of an electric field ($\varepsilon = 50$ V cm^{-1}) we have found an increase in the Ly-α intensity only in the cases of H_2, HD and D_2. This means that only for these three molecules the 2s state is produced in the dissociative excitation process. The 2s cross sections are also given in table 2 together with the 2s/2p cross section ratios.

The experimental results of other groups at 100 eV have been included in table 2 as well.

In fig. 4 the excitation curves of Ly-α ($2p \rightarrow 1s$) radiation are shown for 0 - 100 eV electrons on HCl, H_2O, NH_3 and CH_4. In the case of H_2, D_2 and HD we noticed a large contribution of excited molecular triplet states to the observed radiation for electron energies in the threshold region. This additional radiation may be due to the $a^3\Sigma^+_{(g)} \rightarrow b^3\Sigma^+_{(u)}$ transition, a continuum radiation which can enter our v.u.r. detector system above 1795 Å. Therefore we have omitted the excitation curves for these molecules in fig. 4 because at low incident electron energies the radiation does not refer to Ly-α. For the shape of the Ly-α (H_2) excitation curve see ref. [12]. The same data as presented in fig. 4, are shown in table 3, but now on an absolute scale. Below 100 eV no H,D (2s) cross sections have been measured because of the reasons given in section 2.1.

Our experimental thresholds for Ly-α radiation have been collected in table 4, together with those obtained by some other groups. In the case of HCl and H_2O we have found two clearly observable onsets in each excitation curve. For NH_3 and CH_4 only one onset could be detected clearly.

It has been noticed that the shapes of the Ly-α curves showed similarities with the corresponding ones for Balmer emission [22 - 24].

The $\sigma_{em}(2p \rightarrow 1s)$'s for the incident electron energy range 100 - 2000 eV are collected in table 3. In the case of H_2, HD and D_2 the 2s cross sections are also presented in that table. In fig. 5 some $\sigma_{em}(2p \rightarrow 1s)$ data are shown in the form of Fano plots [25].

TABLE 4

Measured onsets (eV) for Ly-α radiation

com-pound	Observed onset energies (eV)					
	this work	refs.[5-7]	ref.[10]	ref.[11]	ref.[12]	*)
CH_4	20.0 ± 1	21.9	21.9	19 ± 2	-	14.7
NH_3	-	16.1	-	-	-	14.6
	22.0 ± 1	21.8	22.6	22 ± 2	-	
H_2O	17.0 ± 1	16.1 ± 0.5	15.4	15 ± 1	-	15.3
	-	21.5 ± 0.8	-	-	-	
	25.0 ± 1	26.2 ± 1.5	24.0	24 ± 2	-	
	-	ca 40	-	-	-	
HCl	17.0 ± 1	-	-	-	-	14.7
	25.2 ± 1	-	-	-	-	
H_2	-	-	-	-	16.1 ± 2	14.7
	-	-	-	-	27 ± 2	

*) Calculated minimum required energies for H(n=2) production.

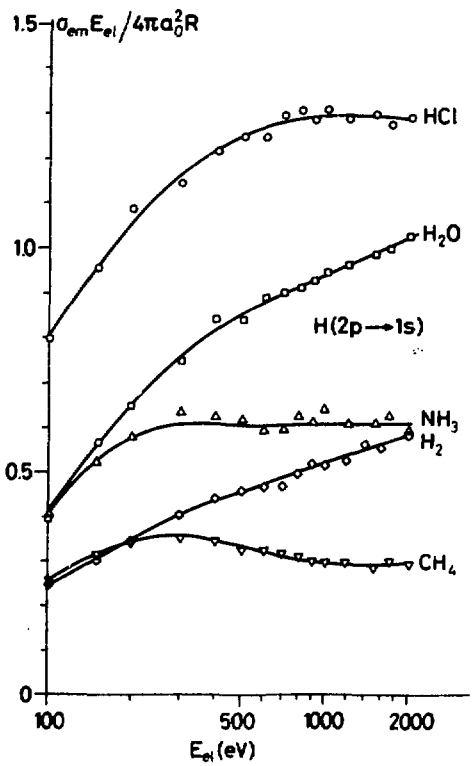

Fig. 5.

Fano plots of Ly-α emission cross sections for 100 - 2000 eV electrons incident on various molecules.

For an introduction and interpretation of the Fano plots see ref. [26] and our previous work [22]. The M_{em}^2 and c_{exc} values derived from such plots are given in table 5, together with previous results of our group.

5. COMPARISON WITH THE RESULTS OF OTHER GROUPS

5.1. 100 eV

First we compare the results for dissociative excitation leading to H(2p).

In the case of 100 eV electrons on H_2, almost all relevant groups have normalized their cross section data for Ly-α ($2p \rightarrow 1s$) emission to that of Fite and Brackmann [1] (corrected for molecular contributions, see our section 2.2), except in ref. [9]. Therefore the $\sigma_{em}(2p \rightarrow 1s, H_2)$'s reported in refs. [3,11] and in the present work are almost the same. De Heer and Carriere [9] have performed cross section calculations for the H_2 Werner bands. to calibrate their optical detection system. Their [9] $\sigma_{em}(2p \rightarrow 1s, H_2)$ result is in good agreement with those in refs. [3,11] and ours. In the case of D_2 we have normalized our $\sigma_{em}(2p \rightarrow 1s)$ data at 100 eV to that of Vroom and de Heer [3].

For CH_4 our σ_{em} value is in good agreement with those of Vroom and de Heer [2] and of McGowan et al. [11]. In all other cases there are discrepancies between our data and those presented in refs. [4-7,10,11]. The discrepancies with the results of refs. [5-7] are probably due to their method of calibration. They have calibrated their optical detection system only at the position of the He (584 Å) line and estimated the quantum yield at 1215 Å. McGowan et al. [11] stated that their σ_{em}'s may be wrong by a factor of two due to the target density determination in that experiment. The discrepancies between our σ_{em} results and those of Morgan and Mentall [10] are not well understood because they have used in principle the same normalization (to ref. [1]) as we did. However, their $\sigma_{em}(2p \rightarrow 1s; CH_4)$ is even lower than $\sigma_{em}(n = 3 \rightarrow 2,1; CH_4)$ as presented in refs. [2,23], which suggests that the values of ref. [11] are unreliable. The discrepancy between our data and that of Vroom and de Heer [4] for H_2O is probably due to the target gas density determination in their experiment as explained in ref. [22].

TABLE 5

M^2_{em} and c_{exc} values for the parent molecules H_2, HD, D_2 and H_2O

	H_2				HD				D_2				H_2O	
	2p → 1s		2s → 1s		2p → 1s		2s → 1s		2p → 1s		2s → 1s		2p → 1s	
	M^2_{em}	c_{exc}	M^2_{em}	c_{exc}	M^2_{em}	c_{exc}	M^2_{em}	c_{exc}	M^2_{em}	c_{exc}	M^2_{em}	c_{exc}	M^2_{em}	c_{exc}
this work	0.0911	$3.95^{+0.73}_{-0.61}$	0.0547	3.90	0.0801	5.08	0.0467	1.43	0.0534	10.1	0.0267	10.0	0.120	34.7
ref. 3	0.120	1.80	0.0572	2.38					0.0839	3.91	0.0411	4.68	0.151	89.3
ref. 8	0.118													

In the case of the 2s cross sections our values agree reasonably with those of Vroom and de Heer [3] for H_2 and D_2. For CH_4 they [2] found a relatively small 2s cross section where we have found the value zero. The value for the 2s cross section reported by Cox and Smith [13] in the case of D_2 is about 40% lower than ours. We have no explanation for this difference.

5.2. 0 - 2000 eV

The measured onset energies for Ly-α ($2p \rightarrow 1s$) radiation agree well with those obtained by the other groups in the case of CH_4, NH_3 and H_2O (see table 4). However in refs. [6,7] more onsets have been reported for Ly-α from H_2O and NH_3 than generally found by the other groups [10,11] and by us.

The shapes of the Ly-α ($2p \rightarrow 1s$) excitation curves for CH_4, NH_3, H_2O and H_2 agree fairly well with those reported in refs. [2-6,10,11] for the relevant electron energy ranges (see table 1). However in the case of NH_3, Böse and Sroka [6] found relatively higher σ_{em}'s than we have found for increasing incident electron energies (45% at 400 eV). In the case of D_2 our σ_{em}'s are relatively lower than those of Vroom and de Heer [3] for increasing electron energies. No data concerning HD have been published elsewhere.

In the case of the 2s cross sections our excitation curves for H_2 and D_2 have a similar shape as the corresponding ones presented in refs. [3,13] for the relevant incident electron energies.

6. DISCUSSION

6.1. H,D(2s,2p) excitation

A striking feature of this study is that, for most of the parent molecules except H_2, HD and D_2, no H atoms in the 2s state are produced by dissociative excitation with electrons. In another study Möhlmann et al. [15] have found that, for electrons on H_2, HCl, H_2O, NH_3 and CH_4, no H(3p) particles are formed. We have no explanation for this yet.

It is interesting to note that only in those cases (H_2, HD and D_2) in which the minimum required energy to produce H(n=2) is smaller than the ionization potential of the parent molecules, H(2s) atoms are produced.

6.2. H_2, HD and D_2

The positive slope in the Fano plot found in the case of H_2 (see fig. 5), HD and D_2 for the formation of H,D(2s,2p) atoms, indicates that optically allowed excitations in the parent molecule play a role in this dissociative process. This means that also via photodissociation of these parent molecules, H(n=2) can be produced. This has indeed been found by several groups, see for instance refs. [27,28] and the relevant references therein. From the slope of the linear part in the Bethe plot the M_{em}^2 value can be obtained. An extensive discussion and interpretation of this value in the case of H_2 and D_2 is given by Vroom and de Heer [3] and therefore does not need to be repeated here.

Because our experimentally obtained c_{exc} values for H_2 and HD are of the order of unity, the contribution of optically allowed excitations is important with respect to symmetry forbidden excitations. For D_2 the c_{exc} value is larger than for H_2 and HD. So in the case of D_2 the symmetry forbidden transitions may contribute relatively more to the production of D(2s,2p) than those in H_2 and HD to the H,D(2s,2p) formation.

From the photodissociation experiments [27,28] it appeared that H(n=2) particles can be produced both by direct dissociation and predissociation of bound Rydberg states converging to the electronic ground state of H_2^+. Misakian and Zorn [14] have shown that in the case of H(2s) split from H_2, besides slow H(2s) atoms (originating from the above mentioned bound Rydberg states) also atoms with a high kinetic energy are produced. These fast atoms may originate from the repulsive doubly excited states with a vertical excitation energy around 29 eV. They [14] give an extensive discussion of the H_2 states which may be involved in the H(2s) formation. Möhlmann and de Heer [29, and references therein] have found that in the case of H($n \geq 3$) production two onsets (ca 18 and 27 eV) are clearly present. These two onsets are probably due to the same type of excitations as indicated above. So it appears from their work [14,29] that, besides singly excited states, the doubly excited states play a role in the formation of H,D* atoms.

6.3. H_2O

The positive slope in the Fano plot shows that optically allowed excitations contribute to the formation of H(2p) atoms. For a discussion of the experimentally obtained M_{em}^2 value, see Vroom and de Heer [4, section IV] who found M_{em}^2 to be of the same order as in the present work. The contribution of optically allowed excitations to the formation of H(2p) has been confirmed by photodissociation experiments of H_2O into H(n=2) and $OH(X^2\Pi_i)$ as performed by Beyer and Welge [30], Guyon et al. [31] and N. Böse et al. [32]. In their work water states with excitation energies between ca 15.3 - 20 eV [30-32] and around 24 eV [31,32] are found to be involved in this dissociation process. These two energy ranges agree with our experimentally observed thresholds (see table 4). The excitation curves for Ly-α and Balmer emissions, obtained in the present work and in ref. [22] respectively for electrons on water, have a similar shape. Therefore H atoms with n=2 and $n \geq 3$ may be produced via the same mechanism In the case of H(n=3) Beenakker et al. [22] have explained that the first threshold may be due to excitation to Rydberg states converging to the third ionization potential of H_2O followed by predissociation via a repulsive doubly excited state. The structure observed in the Ly-α photofluorescence curve between 15.3 - 20 eV of refs. [31,32] suggests that predissociation of the same type of Rydberg states takes place here too. Following Beenakker et al. [22] the second onset at about 25 eV may be due to direct excitation to a repulsive doubly excited state, dissociating into H(n=2) and $OH(X^2\Pi_i)$. Neglecting the correlations between the electrons, simultaneous excitation of two electrons is a symmetry forbidden transition, and is therefore expected not to be important in the photodissociation process. This is consistent with the relatively small Ly-α photofluorescence yield above 24 eV as found in refs. [31,32],and with the relatively large c_{exc} value obtained from our H_2O Fano plot (fig. 5) which indicates that symmetry forbidden excitations contribute significantly to the H(n=2) production by electron impact on H_2O.

6.4. NH_3

In the case of NH_3 it is seen that the slope of the Fano plot (fig. 5) is equal to zero. This means that symmetry forbidden excitations dominate in the production of H(2p). This is consistent with the fact that Beyer and Welge [30] have found only a small Ly-α photofluorescence cross section for NH_3 in comparison with those for H_2 and H_2O. Böse et al. [32] have reported that the photodissociation of NH_3 yielding H(n=2) starts already at the photonenergy of 14.7 eV. However, this onset is not seen in the electron impact experiment. The domination of symmetry forbidden transitions in the production of Ly-α (2p → 1s) radiation is consistent with Ly-α photofluorescence results as explained below. In the photofluorescence spectrum there are two photon energy regions for Ly-α radiation, one starting at 14.7 eV and the other starting at 21 eV. The Ly-α fluorescence intensities are weak (small photofluorescence cross sections for Ly-α). Because we do not see any radiation between 14.7 and 21 eV for electron impact it is probable that also above 21 eV impact energy no Ly-α radiation due to optically allowed transitions will be observed by us. The onset at 22 eV in our experiment must then be mainly due to symmetry forbidden transitions in NH_3 which is consistent with our results from the Fano plot.

Our experimental threshold of 22 eV lies about 7 eV above the minimum required energy for formation of H(n=2). This may mean that H(n=2) is produced together with NH_2 via excitation of a strongly repulsive state, or that total dissociation into the fragments H(n=2) + 2 H(n=1) + N takes place. Wight and Van der Wiel [33] have found that the formation of H^+ from NH_3 starts at about 25 eV which is also 7 eV above the minimum required energy to produce H^+. They [33] explained that the H^+ production proceeds mainly via the repulsive second excited NH_3^+ state. Similarly we may say that the H^* fragments are produced via the repulsive Rydberg states converging to this second excited NH_3^+ state. However, it is strange that all the relevant Rydberg states, which dissociate into H^* and NH_2, are symmetry forbidden with respect to the NH_3 ground state. One then might think that the symmetry forbidden character of the excitation is due to intermediate doubly excited states instead of singly excited Rydberg states. We know that in the case of H_2 doubly excited states

play an important role in the H^* formation (see ref. 29) and that excitation to doubly excited states become more important for increasing number of electrons in the molecule.

6.5. CH_4

As in the case of NH_3, also for CH_4 a symmetry forbidden excitation character has been found for the Ly-α excitation curve.

Only one onset for Ly-α radiation is seen in fig. 4 at about 20 eV which is about 5 eV higher than the minimum required energy for this process. Assuming that H(n=2) and H($n \geq 3$) particles are formed via the same mechanism we can follow the explanation which has been given by Beenakker and de Heer [34] in the case of Balmer radiation from CH_4. They [34] suggest that H^* fragments are produced via excitation of repulsive Rydberg states converging to the second ionization potential (first excited CH_4^+ state) of CH_4 at 23.1 eV. Since symmetry forbidden excitations dominate in the Ly-α production process, one might think again about the importance of the doubly excited states, as in the case of NH_3. Backx and Van der Wiel [35] have found that H^+ ions are formed via excitation of the first excited $(2s_1)^{-1}$ state of CH_4, and also via excitation of an excited CH_4^+ state which can be reached only by a two electron transition at about 30 eV. Rydberg states converging to this latter (symmetry forbidden) excited CH_4^+ state may be involved in the H^* production.

6.6. HCl

Also in this case (see fig. 5) mainly symmetry forbidden excitations in HCl contribute to the Ly-α formation. Two onsets for Ly-α radiation are present at about 17 and 25 eV. The first onset lies about 2.3 eV above the calculated minimum dissociation energy of HCl into H(2p) and Cl(^{2}P). From the combination H(2p) and Cl(^{2}P) six singlet and six triplet states (with Σ^+, Σ^-, Π and Δ symmetries) arise. Some of these states may be repulsive.

The appearance of the first onset at about 17 eV may be explained to be due to:

a) direct excitation above the dissociation limit to the repulsive part of bound states electronically correlated with H(2p) and Cl(^{2}P).

b) predissociation of (vibrationally excited) Rydberg states, converging to the second ionization potential (HCl^+, $A^2\Sigma^+$) of HCl, by the relevant repulsive state.

The second onset at about 25 eV may be due to direct excitation to strongly repulsive (doubly) excited states. The fact that at least a part of the excited H atoms are produced via excitation of these latter strongly repulsive (doubly excited) states has been proved by Ogawa et al. [36] in the case of H(n=4) by Doppler broadening of the Balmer-β emission line. They showed that H(n=4) fragments are produced with translational energies of 7.3 eV by 300 eV electron impact on HCl.

REFERENCES

[1] W.L. Fite and R.T. Brackmann, Phys.Rev. 112 (1958) 1151.
[2] D.A. Vroom and F.J. de Heer, J.Chem.Phys. 50 (1969) 573.
[3] D.A. Vroom and F.J. de Heer, J.Chem.Phys. 50 (1969) 580.
[4] D.A. Vroom and F.J. de Heer, J.Chem.Phys. 50 (1969) 1883.
[5] W. Sroka, Z.Naturforsch. 24a (1969) 1724.
[6] N. Böse and W. Sroka, Z.Naturforsch. 26a (1971) 1491.
[7] N. Böse and W. Sroka, Z.Naturforsch. 28a (1973) 22.
[8] F.J. de Heer, H.R. Moustafa Moussa and M. Inokuti, Chem. Phys.Letters 1 (1967) 484.
[9] F.J. de Heer and J. Carriere, J.Chem.Phys. 55 (1971) 3829.
[10] H.D. Morgan and J.E. Mentall, J.Chem.Phys. 60 (1974) 4734.
[11] J.W. McGowan, J.F. Williams and D.A. Vroom, Chem.Phys.Lett. 3 (1969) 614.
[12] M.J. Mumma and E.C. Zipf, J.Chem.Phys. 55 (1971) 1661.
[13] D.M. Cox and S.J. Smith, Phys.Rev. A 5 (1972) 2428.
[14] M. Misakian and J.C. Zorn, Phys.Rev. A 6 (1972) 2180.
[15] G.R. Möhlmann, S. Tsurubuchi and F.J. de Heer, Chem.Phys. 18 (1976) 145; Chapter II, part A3, of this thesis.
[16] K. Watanabe, Advances in Geophysics 5 (1958) 153.
[17] H. Friedman, Physics of the Upper Atmosphere, J.Ratcliffe Ed. (Academic Press, N.Y., 1960).
[18] J. Carriere and F.J. de Heer, J.Chem.Phys. 56 (1972) 2993.

[19] W.L. Wiese, M.W. Smith and B.M. Miles, Atomic Transition Probabilities (Nat.Bureau of Standards, Washington, 1969).

[20] H.A. Bethe and E.E. Salpeter, Quantum Mechanics of One and Two Electron Atoms (Springer, 1957).

[21] G. Lüders, Z.Naturforsch. 5a (1950) 608.

[22] C.I.M. Beenakker, F.J. de Heer, H.B. Krop and G.R. Möhlmann, Chem.Phys. 6 (1974) 445.

[23] J.F.M. Aarts, C.I.M. Beenakker and F.J. de Heer, Physica 53 (1971) 32.

[24] G.R. Möhlmann, unpublished.

[25] U. Fano, Phys.Rev. 95 (1954) 1198.

[26] M. Inokuti, Rev.Mod.Phys. 43 (1971) 297.

[27] J.E. Mentall and E.P. Gentieu, J.Chem.Phys. 52 (1970) 5641.

[28] P.M. Gluyon and J.E. Mentall, Abstracts of Papers, IX ICPEAC Seattle, eds., J.S. Risley and R. Geballe, Vol.I (1975) p.10.

[29] G.R. Möhlmann and F.J. de Heer, Chapter II, part A1, of this thesis.

[30] K.D. Beyer and K.H. Welge, Z.Naturforsch. 22a (1967) 1161.

[31] P.M. Guyon, J.E. Mentall and G.R. Möhlmann, unpublished.

[32] N. Böse, J. Harms, H. Herz, H. Oertl, H. Schenk, W. Sroka and R. Ziets, Abstracts of Papers, IX ICPEAC, Seattle, eds. J.S. Risley and R. Geballe, Vol. 1 (1975) p.123.

[33] G.R. Wight and M.J. van der Wiel, to be published.

[34] C.I.M. Beenakker and F.J. de Heer, Chem.Phys. 7 (1975) 130.

[35] C. Backx and M.J. van der Wiel, J.Phys.B 8 (1975) 3020.

[36] T. Ogawa, F. Masumoto and N. Ishibashi, Chemistry Letters (1976) 207.